Mechanism of Nitrosylmyoglobin Autoxidation: Temperature and Oxygen Pressure Effects on the Two Consecutive Reactions

Jens K. S. Møller and Leif H. Skibsted*[a]

Abstract: As shown by singular value decomposition and global analysis of the absorption spectra, oxidation of nitrosylmyoglobin, $MbFe^{II}NO$, by oxygen occurs in two consecutive (pseudo) first-order reactions in aqueous air-saturated solutions at physiological conditions (pH 7.0, $I = 0.16$ M (NaCl)). Both reaction steps have a large temperature dependence with the following activation parameters: $\Delta H_1^{\neq} = 121 \pm 7$ and $\Delta S_1^{\neq} = 23 \pm 29$; and $\Delta H_2^{\neq} = 88 \pm 14\ kJ\,mol^{-1}$ and $\Delta S_2^{\neq} = -63 \pm 51\ J^{-1}K^{-1}mol^{-1}$ at 25 °C for the first and second step, respectively. At physiological temperature, the initial reaction is faster, while at lower temperatures, the first reaction is slower and rate-determining. The rate of the first reaction is linearly dependent on oxygen pressure at lower pressures, while for oxygen pressures above atmospheric, the rate exhibits saturation behaviour. The second reaction is independent of oxygen pressure. The rate of the second reaction increases when oxymyoglobin is added. In contrast, the rate of the first reaction is independent of the presence of oxymyoglobin. The observed kinetics are in agreement with a reaction mechanism in which the nitric oxide that is initially bound to the Fe^{II} centre of myoglobin is displaced by oxygen in a reversible ligand-exchange reaction prior to an irreversible electron transfer. The ligand-exchange process is dissociative in nature and depends bond breaking, and nitric oxide is suggested to be trapped in a protein cavity. The absorption spectrum of the intermediate, as resolved from the global analysis, is in agreement with a peroxynitrite complex, and the initial process must involve partial electron transfer.

Keywords: heme proteins · ligand exchange · nitric oxide · nitrosylmyoglobin · reaction mechanisms

Introduction

Mice without myoglobin, which are obtained by gene-knockout, have been found to be viable and even fertile, although their heart and skeletal muscles completely lack pigmentation.[1,2] This intriguing finding may shed doubt on the physiological role of the monomeric heme protein, myoglobin, as being solely an oxygen carrier and storage protein in mammalian tissue. Moreover, later studies have identified multiple compensatory mechanisms in specific heart and blood circulation parameters in transgenic mice devoid of myoglobin.[3,4]

Various forms of myoglobin readily react with nitric oxide (NO) at the iron centre of the protein. The efficient scavenging of free NO by oxymyoglobin ($MbFe^{II}O_2$) has, within the last few years, received increased attention because of the possible effect that this may have in protecting mitochondrial cytochromes in the respiratory system.[5–7] The rate constant for binding NO to Fe^{II} in cytochrome a_3 is reported to be $0.4–1.0 \times 10^8\ M^{-1}s^{-1}$.[8] This is close to diffusion control, and even nanomolar levels of NO may result in instantaneously reversible inhibition of the respiratory system, while higher levels of NO result in irreversible inhibition.[9] $MbFe^{II}$ binds NO with a comparable rate constant of $1.7 \times 10^7\ M^{-1}s^{-1}$, and since $MbFe^{II}$ is present in relatively high concentrations (0.11–0.34 μM), the rate becomes competitive.[10] The fact that Fe^{II} in the heme protein has a high affinity to form very stable complexes, and that NO is oxidised very quickly by oxymyoglobin ($MbFe^{II}O_2$)(second-order rate constant of $3.4 \times 10^7\ M^{-1}s^{-1}$), may be important for the scavenging of NO when this small messenger molecule is produced in excess.[11] Accordingly, regulation of the free NO levels in cardiac, skeletal, or smooth-muscle tissue may depend strongly on myoglobin.[12]

Besides the protective role that myoglobin plays in preventing NO toxicity, as well as regulating the level of free NO, the nitrosylated form of Fe^{II} myoglobin ($MbFe^{II}NO$) may also be an effective antioxidant that prevents lipid per-

[a] Assistant Prof. Dr. J. K. S. Møller, Prof. Dr. L. H. Skibsted
Food Chemistry, Department of Dairy and Food Science
Royal Veterinary and Agricultural University
Rolighedsvej 30, 1958 Frederiksberg C (Denmark)
Fax: (+45) 3528-3344
E-mail: jemo@kvl.dk
ls@kvl.dk

 DOI: 10.1002/chem.200305368

oxidation. The complex $MbFe^{II}NO$ was first identified as the primary pigment in cured meat products, in which it is formed by the concerted reaction of nitrite ion and $MbFe^{II}O_2$ with endogenous or added reductants.[13] Although NO may prevent the pro-oxidative activity of certain forms of myoglobin, the formation of $MbFe^{II}NO$ in vivo has received little attention.[14] Nitric oxide seems to act both as a pro-oxidant and an antioxidant in biological systems, whereas $MbFe^{II}NO$ effectively prevents lipid peroxidation through radical scavenging both in cured meat products and in model systems.[15,16]

Arnold and Bohle have studied the oxygenation reaction of $MbFe^{II}NO$ both at 37 °C and in an atmosphere saturated with pure oxygen.[17] The reaction between $MbFe^{II}NO$ and oxygen is best described by two consecutive reactions that correspond to a bi-exponential expression, and the calculated spectrum of the reaction intermediate indicates that $k_1 < k_2$, in agreement with the spectrum obtained for the intermediate, which resembles a spectrum obtained for an Fe^{III} form of myoglobin, and the authors proposed that the intermediate was a peroxynitrite complex with an N-bound peroxynitrite ligand.

Under physiological conditions, the reaction of NO with $MbFe^{II}O_2$ and the reaction of O_2 with $MbFe^{II}NO$ yields, as common products, $MbFe^{III}$ and nitrate ions. However, the reaction rate is different by several orders of magnitude.[18,19] Although both reactions are of key interest to gain an understanding of the bioregulatory role of NO and myoglobin, the $MbFe^{II}NO$ and O_2 reaction mechanism, in particular, is poorly understood. This has warranted the present kinetic investigation, in which it has been confirmed that autoxidation is a stepwise reaction. In particular, we set out to identify the nature of each of the rate-determining steps in the complex reaction sequence based on the activation parameters derived from the temperature dependence of the reaction rates and on the oxygen pressure dependence.

Results

Nitrosylmyoglobin is slowly oxidised by oxygen in air-saturated aqueous solutions. Moreover, as shown by spectroscopy and electrochemical methods, the oxidation products are metmyoglobin and nitrate ions [Eq. (1)].[17,19]

$$MbFe^{II}NO + O_2 \rightarrow MbFe^{III} + NO_3^- \quad (1)$$

In the present study, the reaction was monitored spectrophotometrically under various conditions relevant for biological systems, and the heme oxidation product was confirmed to be $MbFe^{III}$ (cf. Figure 1 and Figure 3). The observed spectral changes at 20 °C and atmospheric air saturation for wavelengths recorded at appropriate intervals produced the "landscape" illustrated in Figure 1. However, the

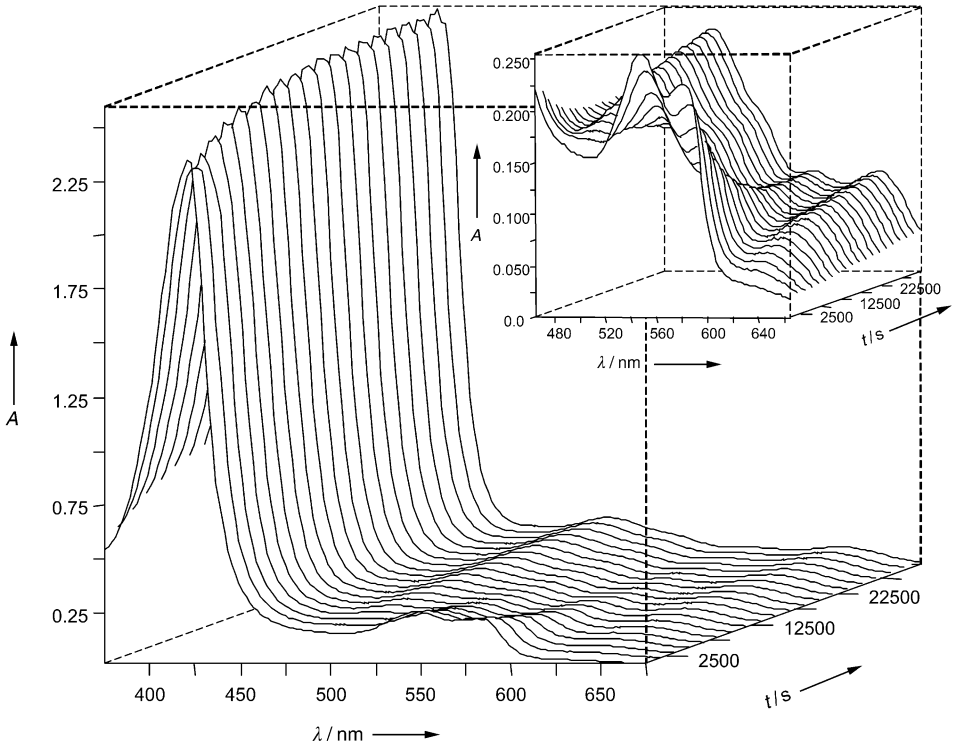

Figure 1. Observed changes in spectral data during autoxidation of nitrosylmyoglobin in air-saturated aqueous solutions (pH 7.0, $I = 0.16$ M) at 20 °C. Initial concentration of nitrosylmyoglobin was approximately 20 μM. The whole spectral landscape was scaled to accommodate the intense Soret band, while the inset diagram shows spectral changes at the β- and α-bands between $470 \leq \lambda \leq 650$ nm in detail. A = absorbance.

kinetics of the autoxidation reaction were not accommodated within the scheme of a single first-order process, as was previously suggested.[19,20] As is evident from Figure 2, which shows the basic spectra and time profiles obtained from U and V matrices, respectively, singular value decomposition (SVD) of spectral changes in the 390–650 nm range (includes the Soret band and the so-called β- and α-band in the visible region) confirmed that in all cases decomposition gives rise to three components. The initial four components clearly illustrate that the fourth component holds no relevant information with respect to both the spectral and time course, while the three preceding components resemble either the Soret or visible bands in which, as seen from the time courses of the second and third component V vectors, changes occur. Accordingly, autoxidation of $MbFe^{II}NO$ was analysed by a general model that includes two consecutive steps [Eq. (2)].

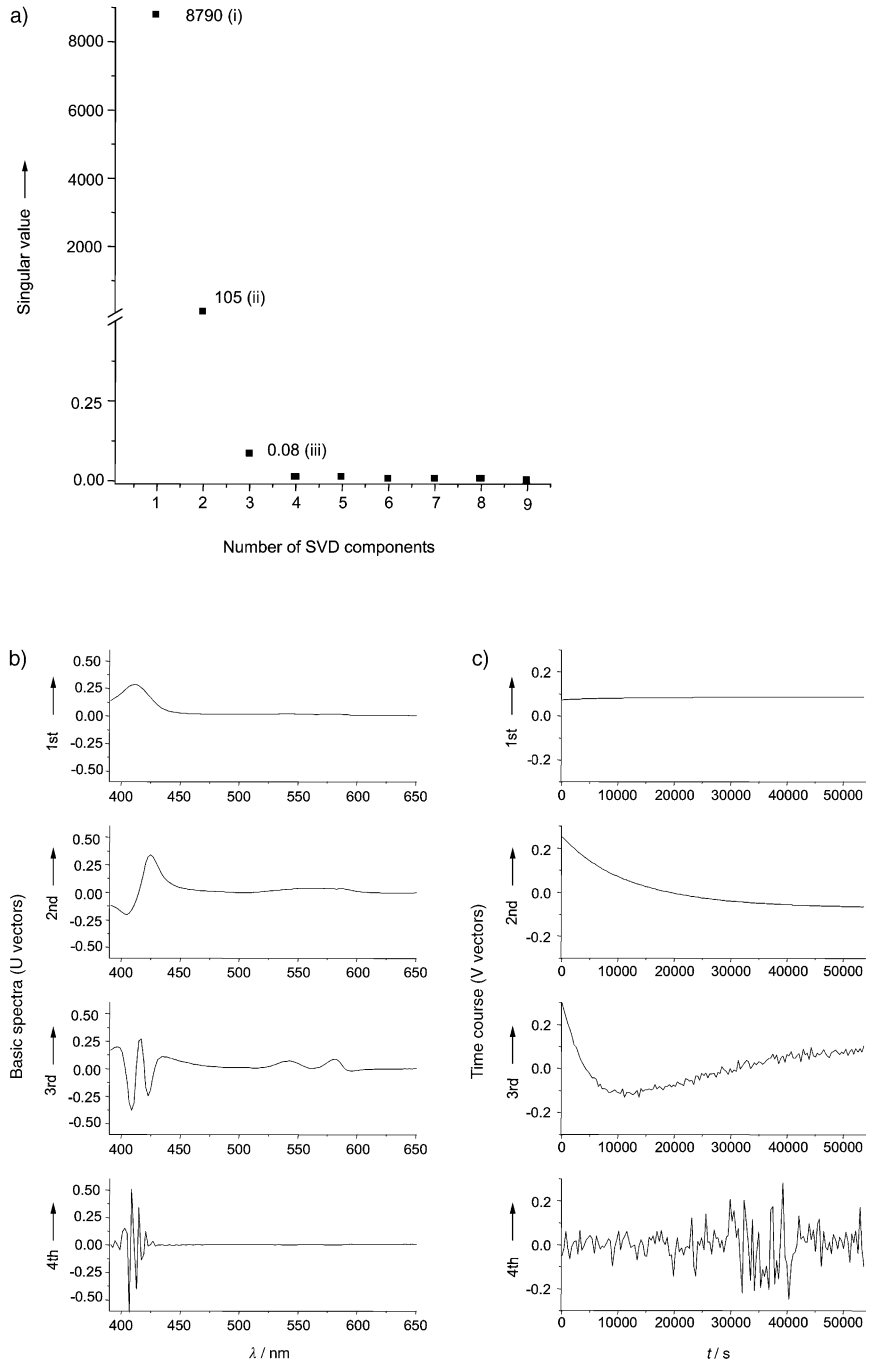

Figure 2. Results from singular value decomposition of spectral data obtained from autoxidation of nitrosylmyoglobin at 15 °C in atmospheric air: a) singular values [with the first three values indicated (i)–(iii)] for SVD components 1–9; b) *U* vectors (basic spectra) for components 1–4; and c) *V* vectors (time course) for components 1–4.

$$MbFe^{II}NO + O_2 \underset{k_{-1}}{\overset{k_1}{\rightleftharpoons}} \text{intermediate} \xrightarrow{k_2} MbFe^{III} + NO_3^- \quad (2)$$

The use of a greater number of wavelengths to estimate the rate constants invariably showed that the reaction could not be described by a single exponential decay, but rather that it consisted of two consecutive reactions; this confirmed the findings made by Arnold and Bohle at 37 °C.[17] The present study was extended over the temperature interval 15–30 °C, and the more powerful numerical method that is now available was utilised. It confirmed that description of the autoxidation process as two (pseudo) first-order reactions [Eq. (2)] was valid over this temperature interval. However, because the two reaction rate constants approach each other in value as the temperature is increased, the numerical calculation became unreliable at higher temperature. Furthermore, both reaction steps may involve a certain degree of reversibility. However, such reversibility, which is most likely to occur in the first reaction step, will not cause any deviation from the (pseudo) first-order kinetics.

The SVD and global analysis of spectral changes during $MbFe^{II}NO$ autoxidation indicated the presence of a reaction intermediate. Moreover, the estimated absorbance spectrum of this reaction intermediate helped to assign the order of the two rate constants. The only reasonable absorption spectrum, which did not have any negative absorption regions, was obtained for $k_1 < k_2$.[21] The estimated absorption spectrum of the reactant $MbFe^{II}NO$, the product $MbFe^{III}$, and the intermediate are given in Figure 3. The absorption spectrum of the intermediate exhibits a higher ε_{max} value than the $MbFe^{III}$ spectrum in the Soret band, but has a similar λ_{max} value to that obtained for $MbFe^{III}$; this is indicative of a ferric heme complex. In the β- and α-band region, four distinct bands can be observed for the intermediate, two of which have high degrees of resemblance to $MbFe^{III}$ (λ_{max}: 505 and 630 nm). The others consist of a shoulder at approximately $\lambda = 548$ nm and a low intensity band at $\lambda = 580$ nm. The reaction intermediate has a similar spectral pattern to transient spectra obtained for a peroxynitrite complex of ferric heme proteins involved in NO-induced oxidation of oxygenated hemoglobin and $MbFe^{II}O_2$.[22,23] In comparison to the spectrum of the intermediate reported by Arnold and Bohle,[17] the spectral pattern in the visible region (β- and α-bands) is in good agreement with the intermediate spectrum found in the

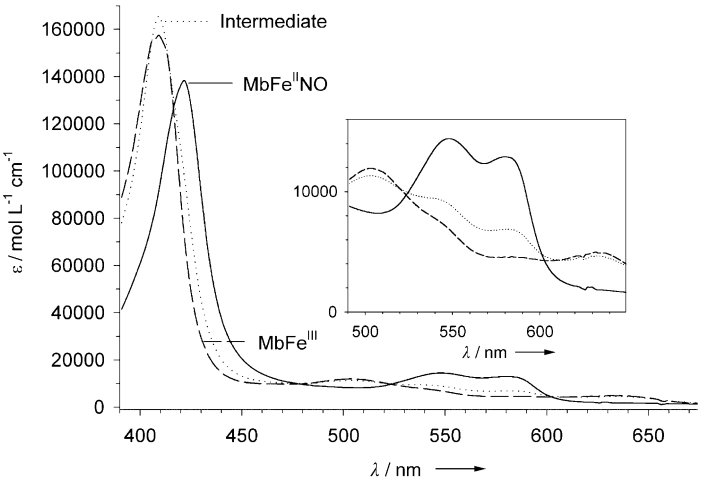

Figure 3. Absorption spectra of MbFe^{II}NO (reactant), MbFe^{III} (product), and an intermediate species during MbFe^{II}NO autoxidation in air-saturated aqueous solutions (pH 7.0, $I=0.16$ M) at 15 °C. The intermediate species exhibits several spectral features similar to a peroxynitrite complex of MbFe^{III} previously described by Herold and Rehmann.[22]

present study. Furthermore, the position of λ_{max} in the Soret band is also in agreement, although the intensity of the Soret bands differ somewhat.

The rate constants for the two consecutive reaction steps in air-saturated aqueous solutions at each of the four temperatures are given in Table 1. As shown in Figure 4, the temperature dependence of the two reactions was analysed according to the Arrhenius equation and non-linear regression. The Arrhenius parameters and transition-state theory also allowed the activation parameters to be calculated (Table 1). The marked difference in the enthalpy of activation for the two reaction steps, which indicates that the first reaction is more sensitive to temperature, makes the concentration profile for the intermediate also strongly dependent on temperature. In particular, maximum concentrations of the intermediate occur at low temperatures. The time profiles for the reactant, the intermediate, and the final product are shown in Figure 5 for the four temperatures studied. At 15 °C as much as 50 % of the total heme protein is present as the intermediate at its concentration peak, while at 30 °C, the maximum intermediate concentration is 20 %. Measurements for the rate of MbFe^{II}NO autoxidation were also performed at 35 °C, but the rate constants were not included in the calculation based on the Arrhenius equation as values for k_1 and k_2 could not be unequivocally assigned in the global analysis of the spectral changes during the reaction. However, in two experiments performed at 35 °C (308.2 K), k_1 and k_2 were found to have average values of $(2.93\pm 0.20)\times10^{-3}\,s^{-1}$ and $(2.86\pm0.66)\times10^{-3}\,s^{-1}$, respectively. Based on the activation parameters contained in Table 1 or the Arrhenius plots in Figure 4, k_1 and k_2 would be expected to be identical and have a value of $1.4\times10^{-3}\,s^{-1}$ at 35 °C. The coalescence of the two rate constants at this particular temperature makes the estimates obtained from the kinetic experiments numerically unreliable, and thus, they were not included in the present calculation of the activation parameters. Moreover, the data obtained at 35 °C could be described by a single exponential expression that nearly had as good a fit as the model, which involved two consecutive reaction steps.

Table 1. Observed (pseudo) first-order rate constants k_1 and k_2 for the two consecutive reaction steps in the autoxidation of MbFe^{II}NO (approximately 2.0 μM) at various temperatures in air-saturated aqueous solutions at pH 7.0 and 0.16 M (NaCl) ionic strength (cf. Figure 1). Activation parameters were calculated by using transition-state theory and Arrhenius parameters (Figure 4).

Variable	k_1 [s^{-1}]	k_2 [s^{-1}]
temperature:		
15 °C ($n=6$)	$(0.73\pm0.31)\times10^{-4}$	$(1.73\pm0.16)\times10^{-4}$
20 °C ($n=4$)	$(1.31\pm0.17)\times10^{-4}$	$(2.59\pm0.21)\times10^{-4}$
25 °C ($n=6$)	$(2.46\pm0.11)\times10^{-4}$	$(3.96\pm0.22)\times10^{-4}$
30 °C ($n=4$)	$(6.23\pm0.22)\times10^{-4}$[a]	$(9.35\pm0.78)\times10^{-4}$[a]
activation parameters:[b]		
$\Delta H^{\neq}$ [kJ mol^{-1}]	120.5 ± 6.8	88.1 ± 14.2
$\Delta S^{\neq}$ [J^{-1}K^{-1}mol^{-1}]	24 ± 29	-64 ± 51

[a] Experimental conditions were identical to those used for measurements of oxygen pressure dependence for $pO_2=21$ %. The rate constants (k_1 and k_2) were not significantly different from those in Table 2 ($P>0.05$), as shown by one-way ANOVA. [b] Standard deviation from the observed rate constants was incorporated as weights in the non-linear regression used to determine the activation parameters.

The autoxidation reaction rate was found to decrease as oxygen pressure decreased. However, as may be seen from the rate constants presented in Table 2, k_2 is independent of oxygen pressure, and only k_1 decreases with decreasing oxygen pressure. Notably, neither k_1 nor k_2 are affected when oxygen pressure is increased from ambient to one atmosphere. The characteristic saturation kinetics observed for the initial step of the reaction sequence may be assigned to the dissociation of nitric oxide in a rate-determining step prior to oxygen being bound at the iron centre. However, as has previously been discussed, the same oxygen dependence would be observed for an associative mechanism, in which oxygen is bound prior to oxidation.[19] The observed value for k_1 in relationship to pO_2, for both mechanisms, is in

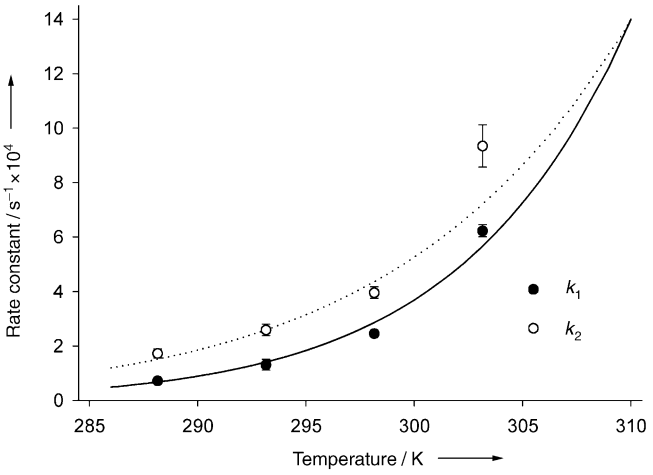

Figure 4. Non-linear regression fit to the Arrhenius equation of the observed (pseudo) first-order rate constants k_1 (●) and k_2 (○) for the two consecutive reactions of MbFe^{II}NO autoxidation in air-saturated ([O_2] varies between 0.32 and 0.24 mM) aqueous solutions (pH 7.0, $I=0.16$ M). The rate constants for each temperature investigated were obtained by global analysis using singular value decomposition of the spectral data, as shown in Figure 1 for 20 °C.

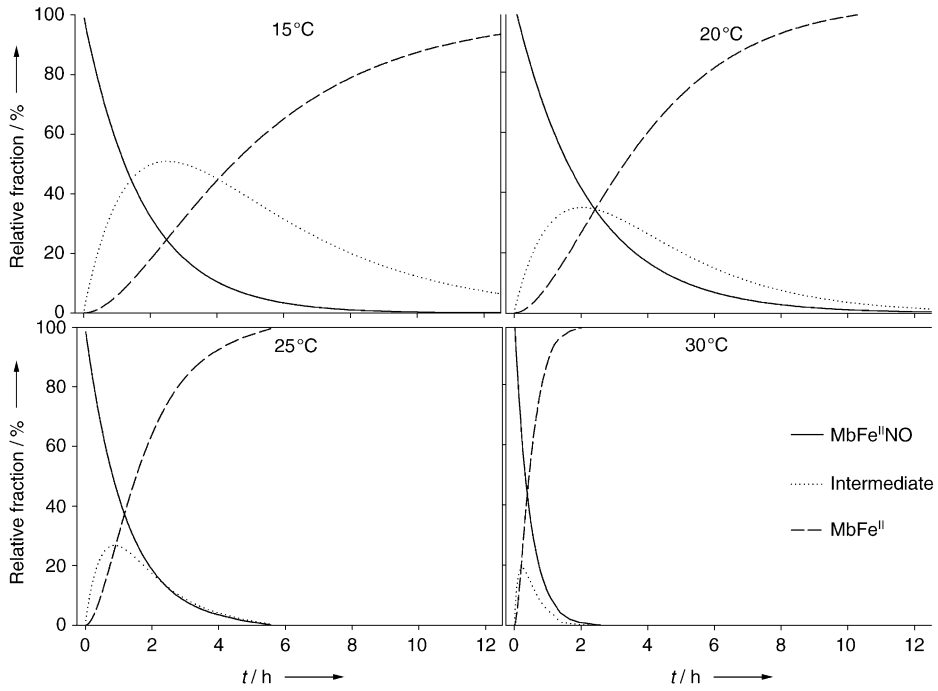

Figure 5. Time profiles for the three species during autoxidation of $MbFe^{II}NO$ to give $MbFe^{III}$ and nitrate ions in air-saturated aqueous solutions (pH 7.0, $I = 0.16$ M) at 15, 20, 25 and 30 °C.

Table 2. Observed (pseudo) first-order rate constants for the two consecutive reaction steps in $MbFe^{II}NO$ autoxidation (approximately 2.0 μM) at various oxygen pressures in aqueous solutions at pH 7.0 and 0.16 M (NaCl) ionic strength. The limiting value and equilibrium constant for ligand exchange was calculated from Equation (3) using non-linear regression analysis.

Variable		k_1 [s^{-1}]	k_2 [s^{-1}]
pO_2:	1% ($n=4$)	$(1.63\pm0.55)\times10^{-4}$	$(8.06\pm0.75)\times10^{-4}$
	10% ($n=3$)	$(4.30\pm0.78)\times10^{-4}$	$(7.13\pm0.61)\times10^{-4}$
	21% ($n=4$)	$(5.90\pm0.86)\times10^{-4}$[a]	$(7.26\pm0.76)\times10^{-4}$[a]
	100% ($n=5$)	$(5.89\pm0.74)\times10^{-4}$	$(6.19\pm0.44)\times10^{-4}$
saturation kinetics for step 1			
maximal rate, $k_{1(max)}$ [s^{-1}]		$(6.20\pm0.04)\times10^{-4}$	
equilibrium constant for ligand exchange, $K_{exchange}$		$(3.00\pm0.9)\times10^{-2}$	

[a] Experimental conditions were identical to those used for measurements of temperature dependence for k_1 and k_2 at 30 °C. The rate constants (k_1 and k_2) were not significantly different from those in Table 1 ($P > 0.05$), as shown by one-way ANOVA.

accord with a two-parameter expression similar to the Michaelis–Menten equation [Eq. (3)].

$$k_1 = \frac{a \times pO_2}{1 + (b \times pO_2)} = \frac{k_{1(max)} \times K_{exchange} \times pO_2}{1 + (K_{exchange} \times pO_2)} \quad (3)$$

In Equation (3), the empirical parameters a and b have been further related to the equilibrium constant for the exchange of NO with O_2 ($K_{exchange}$) [Eq. (4)], and with the rate constant for NO dissociation, which corresponds to a limiting dissociative mechanism for the initial reaction of the sequence [Eq. (5)].

$$MbFe^{II}NO + O_2 \overset{K_{exchange}}{\rightleftharpoons} MbFe^{II}O_2 + NO \xrightarrow{k_2} MbFe^{III} + NO_3^- \quad (4)$$

$$K_{exchange} \approx \frac{k_1 + k_2}{k_{-1}} \quad (5)$$

The numerical value obtained for $K_{exchange}$, which was calculated by non-linear regression analysis of k_1 at 30 °C (Figure 6) according to Equation (3), was found to be $(3.0\pm0.9)\times10^{-2}$ (Table 2). The limiting k_1 value at high oxygen concentrations is $(6.20\pm0.04)\times10^{-4}\ s^{-1}$; this is very similar to the value found for k_2 [$(6.19\pm0.44)\times10^{-4}\ s^{-1}$] at 30 °C and pO_2 of one atmosphere.

In the limiting mechanism described in Equation (4), NO and $MbFe^{II}O_2$ are considered to be formed as reaction intermediates. To test this hypothesis, three types of experiments were conducted.

In the first type of experiment, because the second-order reaction between $MbFe^{II}O_2$ and NO in Equation (4) is known to be dependent on pH and the value of k_2 increases as pH is increased,[22,23] it was considered that an increase in pH from 7.0 to 9.5 should result in an increase in the value of k_2 by a factor of two for the reaction depicted in Equation (6).

$$MbFe^{II}O_2 + NO \xrightarrow{k_2} MbFe^{III} + NO_3^- \quad (6)$$

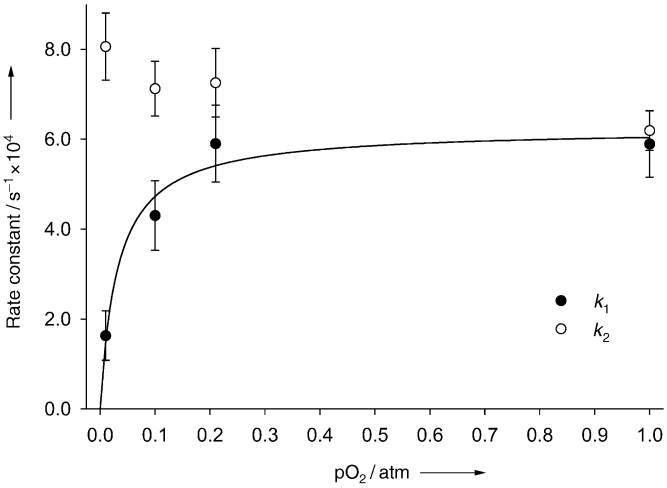

Figure 6. Observed (pseudo) first-order rate constants k_1 (●) and k_2 (○) for the two consecutive reactions of $MbFe^{II}NO$ autoxidation in aqueous solutions (pH 7.0, $I = 0.16$ M) at 30 °C for varying oxygen pressures (11–1130 μM [O_2]). Curves were obtained from fitting the parameters of the first-order rate constant (k_1) for the first reaction step using Equation (3) and non-linear regression. In this manner, the limiting value for k_1 was calculated to be $k_{1(max)} = (6.2\pm0.4)\times10^{-4}\ s^{-1}$, and the equilibrium constant for O_2/NO exchange by $MbFe^{II}NO$ was determined to be $K_{exchange} = 0.030\pm0.009$. The first-order rate constant (k_2) for the second reaction step was found to be independent of pO_2 ($P > 0.05$).

Such an effect was clearly not observed, as in a borax buffer of pH 9.5 at 20 °C, k_1 and k_2 were found to have values of $(9.6 \pm 1.5) \times 10^{-5}$ and $(1.53 \pm 0.32) \times 10^{-4}\ s^{-1}$, respectively. Indeed, the k_1 value was very similar to the value obtained in a phosphate buffer at pH 7.0 [$(1.31 \pm 0.14) \times 10^{-4}\ s^{-1}$, Table 1], while the k_2 value determined at pH 9.5 was even smaller than that found at pH 7.0 [$(2.59 \pm 0.21) \times 10^{-4}\ s^{-1}$, Table 1]. Protein conformation effect, and the fact that the oxidation product is a hydroxide complex of $MbFe^{III}$, which has spectral characteristics in the visible region that are similar to both $MbFe^{II}NO$ and $MbFe^{II}O_2$, may have complicated the numerical resolution of k_1 and k_2.[24] However, it is clear that k_2 does not relate to a bimolecular reaction between NO and $MbFe^{II}O_2$, since an increase in k_2 would have been observed upon changing the pH from 7.0 to 9.5.

For the second type of experiment, any unbound NO should in aqueous solution and in the presence of O_2 undergo a third-order reaction according to Equation (7) with $k = 8.0 \times 10^6\ M^{-2}\ s^{-1}$ to yield nitrite ions.[25]

$$4\,NO + O_2 + 2\,H_2O \rightleftharpoons 4\,NO_2^- + 4\,H^+ \qquad (7)$$

Although a sensitive colorimetric method was used (results not shown), nitrite ions were not detected during $MbFe^{II}NO$ autoxidation at either low (0.01 atm) or high oxygen pressures (1 atm).

For the third type of experiment, $MbFe^{II}NO$ was allowed to undergo autoxidation at 30 °C in the presence of an equimolar amount of $MbFe^{II}O_2$ in order to identify the role that $MbFe^{II}O_2$ plays in the oxidation of NO. Spectral analysis of the reaction mixture during autoxidation of equimolar amounts of $MbFe^{II}NO$ and $MbFe^{II}O_2$ showed a complicated kinetic pattern. As a result, the spectra of pure $MbFe^{II}NO$ and $MbFe^{II}O_2$ were introduced into the SVD global analysis in order to avoid rank deficit and to obtain reliable k_1 and k_2 estimates. Under these conditions the value of k_1 was determined to be $(4.57 \pm 0.20) \times 10^{-4}\ s^{-1}$ ($n = 4$); this is comparable to $(6.23 \pm 0.22) \times 10^{-4}\ s^{-1}$ ($n = 4$, Table 1), which was determined when only $MbFe^{II}NO$ was present in the reaction mixture. Therefore, the rate constant (k_1) for the initial reaction is not significantly altered. In contrast, k_2 was estimated to be $0.13 \pm 0.02\ s^{-1}$ ($n = 4$), which is more than 100-times greater than the k_2 value determined in the absence of $MbFe^{II}O_2$ [$(9.35 \pm 0.78) \times 10^{-4}\ s^{-1}$, $n = 4$, Table 1]. Although the global analysis failed to estimate time profiles for the three species without the spectral restriction described, the rate constants found for mixtures of $MbFe^{II}NO$ and $MbFe^{II}O_2$ are indicative of a mechanism in which an initial NO/O_2 ligand exchange is followed by NO-induced oxidation of $MbFe^{II}O_2$. Therefore, an excess of $MbFe^{II}O_2$ will effect the rate of the second reaction step, as the concentration of substrate available for NO-induced oxidation is elevated. The rate constant (k_{obs}) for autoxidation of $MbFe^{II}O_2$ in air-saturated aqueous solutions (pH 7.0 and $I = 0.16\ M$) at 30 °C has a value of $10^{-5}\ s^{-1}$.[24] From this value it can be calculated that within the time span the reaction is monitored in the present experiment, a maximum 2% of the conversion of $MbFe^{II}O_2$ to $MbFe^{III}$ occurs as a result of autoxidation. Accordingly, the observed increase in rate is the result of $MbFe^{II}O_2$ reacting with NO to yield $MbFe^{III}$ and NO_3^-, or more specifically relates to the second reaction step.

From experimental observations, it can be concluded that autoxidation of $MbFe^{II}NO$ occurs in two steps. The first reaction step involves NO dissociation (NO possibly escapes to internal globin cavities) and subsequent O_2 association to Fe^{II}. This initial, rate-determining step may also include some degree of electron transfer from Fe^{II} in agreement with the Fe^{III} spectrum of the intermediate, while the second step is a reaction in which an O-bound peroxynitrite complex rearranges and dissociates.

Discussion

Studies on recombinant mutant myoglobins, in which specific amino acid residues have been altered to change the environment of the heme pocket, and as a result the ligand accessibility, have shown that NO-induced oxidation of $MbFe^{II}O_2$ depends mainly on the rate of NO entry into the heme pocket.[18] The NO-induced oxidation of $MbFe^{II}O_2$ is fast compared to the oxidation of $MbFe^{II}NO$ by O_2. However, the observation that the mobility of NO in the heme protein cavity is important for subsequent electron-transfer reactions is relevant also for the "reverse" reaction, in which electron transfer occurs when O_2 enters the $MbFe^{II}NO$ heme protein. As was recently discussed in a review that covered NO and myoglobin interactions, a common reaction intermediate for the two reactions in which NO and O_2 are positioned for electron transfer should be considered.[20]

As outlined in Scheme 1, $MbFe^{II}NO$ autoxidation has previously been described by different reaction mechanisms. The four mechanisms are ordered in relation to their degree of associative (top) or dissociative nature (bottom), and can be described as follows: 1) a reaction with two consecutive reaction steps that has the rates k_1' and k_2', respectively, and in which an intermediate is formed upon attack on the nitrogen atom in Fe^{II}–N–O by O_2;[17,19] 2) an initial fast (not observable) association of O_2 to the NO ligand followed by a rate-determining step that involves electron transfer and dis-

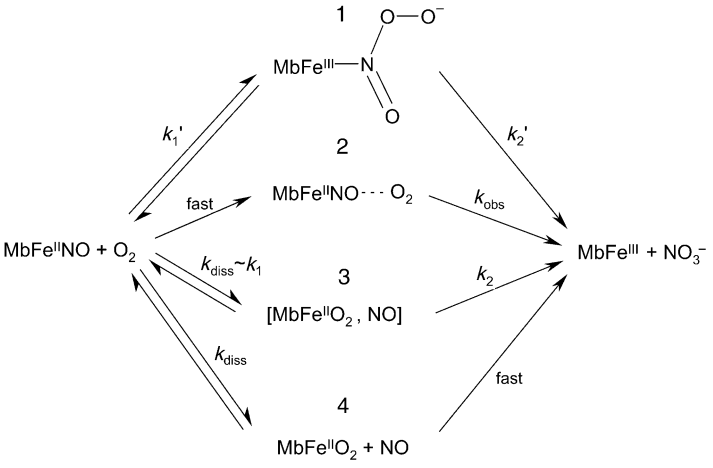

Scheme 1.

sociation from myoglobin (k_{obs});[19] 3) a reaction that corresponds to the mechanism proposed on the basis of the new experiments reported in the present paper and described below; and 4) a reaction that has a limiting dissociative mechanism, and which involves an initial ligand exchange between bound NO and O_2 present in solution. Nitric oxide dissociation is then followed by rapid NO-induced oxidation of $MbFe^{II}O_2$ in a bimolecular reaction, and the observed rate constant (k_{diss}) corresponds to the rate constant for dissociation of NO from $MbFe^{II}NO$.[26] Dissociation of NO from $MbFe^{II}NO$, which is suggested to be rate-determining in the latter mechanism, is a relatively slow process. Indeed, NO trapping techniques at neutral pH and 20 °C have shown the rate of this step to be $1.2\times10^{-4}\,s^{-1}$.[27] In a more recent study, a comparable value of $9.0\times10^{-5}\,s^{-1}$ was obtained under similar conditions.[28]

The NO-induced oxidation of oxygenated heme proteins is fast, and has been the subject of a number of studies during the past few decades.[22,29] In two of the more recent studies, the second-order rate constant for the reaction between $MbFe^{II}O_2$ and NO at neutral pH and 20 °C was estimated to be $3.4\times10^{7}\,M^{-1}s^{-1}$ and $4.4\times10^{7}\,M^{-1}s^{-1}$, respectively.[18,23]

One of the conclusions drawn from the present study is that kinetically, the rather slow reaction between $MbFe^{II}NO$ and O_2 at low temperatures appears to be the result of a two-reaction sequence. At temperatures around 35 °C, the values of the two rate constants approach each other, and in a certain temperature range, the process will appear kinetically as a single reaction. This apparent change from two reactions to one as the temperature is increased may explain the somewhat conflicting kinetics reported for the autoxidation.[17,19,20,26]

The first reaction is characterised by a (pseudo) first-order rate constant that is linearly dependent on oxygen concentration at low concentrations, but which is oxygen independent at higher oxygen concentrations. The second reaction step has a first-order rate constant that is independent of oxygen pressure; this suggests that the first reaction involves some degree of binding of O_2 to $MbFe^{II}NO$, while the second reaction is an intramolecular rearrangement. The generalised reaction shown in Equation (2) accommodates both of the two limiting mechanisms, that is, attack on coordinated NO by O_2 (Scheme 1, 1), as well as complete exchange prior to reaction following an initial NO dissociation (Scheme 1, 4).

The $MbFe^{II}NO$ autoxidation rate has been found to decrease with increasing hydrostatic pressure, corresponding to a positive volume of activation of $\Delta V^{\neq}=+8\,mL\,mol^{-1}$,[30] and indicating that the coordination sphere undergoes expansion in the reaction of $MbFe^{II}NO$ with O_2. Such a volume increase is normally related to a dissociative reaction mechanism. In particular, it would correspond to dissociation of NO from $MbFe^{II}NO$ prior to reaction with O_2 (Scheme 1, 4). However, the mechanism suggested by Arnold and Bohle, which involves an intermediate peroxynitrite complex, could also result in an expansion of the coordination sphere (Scheme 1, 1). Moreover, this mechanism also consists of two consecutive reaction steps, and is similar to the mechanism proposed for the NO-induced oxidation of $MbFe^{II}O_2$. The latter reaction proceeds through the intermediate depicted in Equation (8), in which NO is bound to the heme cavity oxygen.[31] Notably, this intermediate is stabilised under alkaline conditions, that is, when the pH is increased from 7.0 to 9.5.

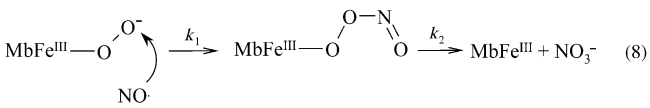

(8)

A similar intermediate to the peroxynitrite complex of $MbFe^{III}$ observed in the reaction of NO with $MbFe^{II}O_2$ also seems to be in agreement with the kinetics observed for the autoxidation. However, the intermediate in the autoxidation is not stabilised by hydroxide and at least the coordination environment may differ. Strong evidence that the rate-determining step in the first reaction is an initial ligand exchange between NO and O_2 has been presented by Eich, who showed that a high correlation ($r^2=0.95$) exists between the rate constant for NO dissociation and the rate constant for autoxidation of NO complexes of 18 myoglobin mutants, each of which is described as a single first-order reaction.[26] It has also been concluded that ligand exchange is the initial step of $MbFe^{II}NO$ autoxidation, and that NO dissociation is rate-determining.

However, isotopic labelling studies found that exchange of bound NO with free NO was faster than NO dissociation from $MbFe^{II}NO$ ($k_{exchange}>10^{-2}\,M^{-1}s^{-1}$).[19,32] Thus, NO exchange and $MbFe^{II}NO$ autoxidation cannot have a common pentacoordinate Fe^{II} intermediate and be purely dissociative in nature. The entering NO molecule in the exchange reaction or the entering O_2 molecule in the autoxidation reaction is more likely to form a transition state or intermediate in which there is some degree of association with the leaving NO. The exchange activation enthalpy for NO in $MbFe^{II}NO$ was found to be $47\,kJ\,mol^{-1}$;[32] this is substantially smaller than the activation barrier found for the autoxidation of $MbFe^{II}NO$[19] (cf. Table 1). Together, these observations suggest that although ligand dissociation is rate-determining for the first reaction step, both ligands are in proximity to the Fe^{II} centre prior to the second reaction step taking place (Scheme 1, 3).

An autoxidation mechanism in which NO initially undergoes dissociation is supported by the fact that the value found for k_1 [$(1.31\pm0.17)\times10^{-4}\,s^{-1}$ at 20 °C, Table 1] is comparable to the rate constant for NO dissociation from $MbFe^{II}NO$ ($1.2\times10^{-4}\,s^{-1}$[27]). The somewhat higher value observed for k_1 possibly arises because of a contribution from the rebinding of NO to $MbFe^{II}$ in the heme cavity. In this case, the observed k_1 value will be equal to $k_{diss}+k_{-1}$. The high second-order rate constant observed for NO-induced oxidation of $MbFe^{II}O_2$ ($3.4\times10^{7}\,M^{-1}s^{-1}$ at 20 °C[18]) is in marked contrast to the value obtained for the first-order rate constant of the second step [$(2.59\pm0.24)\times10^{-4}\,s^{-1}$ at 20 °C]. However, the effective concentration of uncoordinated NO will be extremely low during the autoxidation of

$MbFe^{II}NO$ even for a mechanism in which there is initial ligand exchange. Moreover, NO that has become dissociated and replaced by O_2 may still be present within the protein and will attempt to rebind. In the present study, and in contrast to what was found for the NO-induced oxidation of $MbFe^{II}O_2$, NO present in protein cavities clearly behaves differently to NO present in solution because the reaction intermediate is not significantly stabilised by an increase in pH.

The relatively large activation barrier for step 1 ($\Delta H_1^{\neq} = 121\ kJ\,mol^{-1}$, Table 1) is in agreement with a dissociative mechanism, in which the rate-determining step involves the breaking of the strong NO–Fe^{II} bond. This is followed by a non-activated NO escape into the heme cavity and then further relocation into protein cavities.[33] The second step has an activation barrier of $\Delta H_2^{\neq} = 88\ kJ\,mol^{-1}$, which most likely indicates that electron transfer rather than bond breaking is rate-determining. This is further supported by the negative value obtained for the entropy of activation.

The entropy of activation for the transition state in step 1 is close to zero ($\Delta S_1^{\neq} = 24 \pm 29\ J^{-1}K^{-1}mol^{-1}$), and is thereby in agreement with a dissociative mechanism in which the dissociated NO molecule remains in the heme cleft. The Fe^{II} coordination sphere with NO unbound, but still in close proximity, only gives rise to minor changes in the organisation of the heme pocket. Finally, an electrostatic interaction between the unbound NO and the distal residue His64 may counteract a positive contribution to the entropy of activation for ligand dissociation from $MbFe^{II}NO$. In contrast, the entropy of activation for the second step is negative ($\Delta S_1^{\neq} = -64 \pm 51\ J^{-1}K^{-1}mol^{-1}$). This suggests that an inner-sphere electron transfer takes place between the coordinated O_2 and the NO trapped in the protein cavity to give a peroxynitrite intermediate like the one seen in Equation (8).[23] However, based on the calculated spectrum character alone, it cannot be ruled out that the reaction intermediate is a ferric heme complex of other nitrogen oxides, for example NO_2^- or NO_3^-, as these have a similar spectral pattern.

The observation of kinetic saturation [Eq. (3)] with respect to oxygen concentration for the first reaction step allowed a value to be calculated for the exchange equilibrium constant $K_{exchange}$ [Eq. (5)]. However, because $K_{exchange}$ is also dependent on the rate of further reactions, for example k_2, it resembles the Michaelis–Menten constant and is not a "true" thermodynamic constant. Notably, the rate of NO dissociation from nitrosylated heme complexes was found to exhibit saturation behaviour in the presence of imidazole as the concentration of imidazole was increased.[28]

The equilibrium constant for the exchange of NO with oxygen (K_{NO/O_2}), which is a true equilibrium constant, was estimated from the equilibrium constants for NO and O_2 dissociation from $MbFe^{II}$ (7×10^{-12} M and 7.1×10^{-7} M, respectively)[10] to be approximately 10^{-5}. The difference between the values obtained for K_{NO/O_2} and $K_{exchange}$ indicate that factors such as subsequent reactions contribute to $K_{exchange}$ (cf. [Eq. (4)]), and in effect make $K_{exchange}$ larger than K_{NO/O_2}. This difference illustrates the complexity of the mechanism for $MbFe^{II}NO$ autoxidation, which appears to have a number of intermediates of fleeting existence.

Reaction pathway 3 in Scheme 1 provides the most complete description of the experimental observations. In this mechanism, NO dissociates from Fe^{II}, but remains within the protein and is most likely trapped in a cavity, while O_2 binds to Fe^{II}. The elementary reaction whereby NO undergoes dissociation is somewhat assisted by an entering O_2. This first reaction step has a k_1 very similar to the dissociation rate constant k_{diss}. Dissociation is then followed by oxidation of $MbFe^{II}O_2$, during which time NO is present within the protein cavity, and is therefore, unavailable for reaction in the solvent with non-coordinated O_2. The rate-determining step for the second reaction seems to involve a transition state in which NO establishes contact with the O_2 coordinated to Fe^{II} from within the protein cavity, and an electron is transferred from NO to O_2. This transition state may be identical to the transition state in NO-induced oxidation of $MbFe^{II}O_2$. The significant increase in k_2 observed for equimolar concentrations of $MbFe^{II}NO$ and $MbFe^{II}O_2$ in relation to $MbFe^{II}NO$ alone could indicate that the dissociated NO molecule is trapped in a cavity close to the surface of the protein or that it may even have passed into the solvent, whereby it can react with protein molecules other than the myoglobin it was originally bound to. The reason that nitrite ions are not detected as a result of O_2 oxidation of NO in solution is that this particular reaction is governed by a third-order rate law (second order in [NO]). Thus, in the presence of elevated concentrations of $MbFe^{II}O_2$, only the rate constant for the second step (k_2) is effected.

Under conditions in which tissue fibres have a low oxygen supply, for example ischemia, and in the presence of elevated levels of NO,[34] NO will bind to $MbFe^{II}$ rather than react with $MbFe^{II}O_2$. Under such conditions $MbFe^{II}NO$ has been detected in myocardial tissue.[35,36] Now, apart from $MbFe^{II}NO$ preventing excess free NO from inactivating cytochrome, it is possible that the NO bound to $MbFe^{II}$ acts as a potential antioxidant. Indeed, $MbFe^{II}NO$ has recently been shown to reduce the rate of peroxidation in a lipid model system,[16] while administration of an NO donor during ischemia reperfusion was found to protect against myocardial injury.[37] Alternative roles of Mb have been suggested in cardiovascular biology, including the regulation of NO availability by scavenging and also transportation of the small messenger molecule together with the activity of Mb as a peroxidase.[38] Thus, $MbFe^{II}NO$ may have a function in scavenging reactive oxygen species, as well as other radical species formed during ischemia and oxidative stress. Notably, the mechanism of $MbFe^{II}NO$ autoxidation appears to ensure that NO is not released from $MbFe^{II}NO$ by a ligand-exchange process when normal levels of oxygen have been restored, as the exchanged NO will react with O_2 within the same molecule of myoglobin to form $MbFe^{III}$ and nitrate ions. Although, as also indicated by the experiment with mixtures of $MbFe^{II}NO$ and $MbFe^{II}O_2$, it cannot be excluded that NO molecules will leave the vicinity of the protein in nanomolar concentrations by internal pathways. The proposed concerted reactivity of myoglobin towards NO and O_2 is in agreement with reports published by Fauenfelder et al.[7] These authors suggested that myoglobin was a bio-

chemical reactor that catalyses reactions among small diatomic molecules such as O_2, NO and CO.

Future research into the complex reaction of $MbFe^{II}$ with NO and O_2 should focus on the nature of the transition state in the second reaction step that involves $MbFe^{II}NO$ and O_2, in order to clarify whether this transition state is actually similar to that proposed for the reaction of NO with $MbFe^{II}O_2$ (Scheme 2). The spectra observed for the intermediate in the present studies would indicate that this is the case. It is possible that NO molecules may approach O_2 bound to Fe^{II} from different cavities in the protein for the two reactions, since several myoglobin cavities in which small molecules are kinetically trapped, have been characterised using crystallographic techniques.[39–41] A description of the trajectory of NO molecules into and inside myoglobin may provide insight into the various functions that myoglobin has in regulating the concentration of small molecules in living organisms.

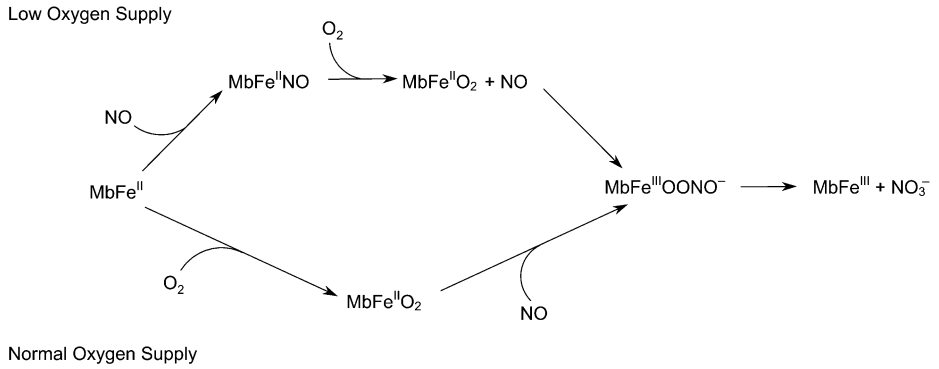

Scheme 2.

In conclusion, $MbFe^{II}$ seems to have a dual function in regulating NO molecule concentrations in mammalian muscle cells (Scheme 2). Under conditions of normal O_2 supply, the oxygenated $MbFe^{II}$ complex in effect becomes a nitric oxide oxidase and ensures the rapid oxidation of NO. On the other hand, in the absence of O_2, $MbFe^{II}$ stores NO possibly as a bioactive reservoir until O_2 once again becomes available for the oxidation of NO. The release of NO in these instances occurs slowly. The marked differences in the rates of the two processes depends on the order in which the two low molecular weight molecules are bound to myoglobin.

Experimental Section

Chemicals: Water was filtered through a Millipore Q-plus purification train (Millipore, MA, USA). Disodium hydrogenphosphate, sodium dihydrogenphosphate, vanadium(III) chloride, sodium dithionite, sodium tetraborate and sodium decahydrate were purchased from Merck (Damstadt, Germany). Sodium nitrite, potassium nitrate, sodium ascorbate, Griess reagent (modified), and metmyoglobin (horse heart, type III) were purchased from Sigma Aldrich (St. Louis, MO, USA). All chemicals were of analytical grade.

Nitrosylmyoglobin and oxymyoglobin synthesis: Aqueous solutions of $MbFe^{II}NO$ were synthesised from an aqueous solution of $MbFe^{III}$ (2×10^{-5} M) in 10 mM phosphate buffer (pH 7.0, $I=0.16$ M (NaCl)). They were subsequently deoxygenated by purging with N_2 and allowed to react under anaerobic conditions in the dark with sodium nitrite and sodium ascorbate (pH 5.0) as previously described.[19] $MbFe^{II}NO$ was purified on a chilled (5 °C) PD10 (Sephadex G-25) column using phosphate (pH 7.0, $I=0.16$ M) or borate buffer (pH 9.5, $I=0.16$ M) as eluent. $MbFe^{II}NO$ was synthesised daily for use in all types of experiments. $MbFe^{II}O_2$ was synthesised by adding 10% sodium dithionite solution to $MbFe^{III}$ (2×10^{-5} M) in 10 mM aqueous phosphate buffer (pH 7.0, $I=0.16$ M). The reaction mixture was subsequently allowed to react with atmospheric oxygen and was purified on a chilled PD10 column as described above.

Kinetic experiments: $MbFe^{II}NO$ autoxidation was monitored for solutions at pH 7.0 (phosphate buffer) or pH 9.5 (borate buffer) at an ionic strength of 0.16 M (NaCl) on either a HP8452A or a HP8453 UV/Vis diode array spectrophotometer (Hewlett Packard, Palo Alto, CA, USA) equipped with both a single and multicell thermostatted cuvette holder, as well as a magnetic stirrer. Spectral changes during kinetic measurements were recorded in the wavelength range $390<\lambda<650$ nm at 2 nm intervals. Conversion of $MbFe^{II}NO$ to $MbFe^{III}$ was followed for a minimum of three reaction half lives at 30, 25, 20, and 15 °C; this corresponds to a 90% conversion.

Partial oxygen pressure (pO_2) was controlled by flushing the reaction mixtures with certified gas mixtures of nitrogen and oxygen (1% or 10% oxygen) obtained from AGA Gas A/S (Copenhagen S, Denmark), atmospheric air, or 100% oxygen when the $MbFe^{II}NO$ solutions were to be saturated (approximately 20 μM). After synthesis and purification, solutions were immediately transferred to a 1-cm long-necked cuvette that could hold 2.5 mL of solution. The cuvette was subsequently sealed with a rubber septum (Sigma Aldrich), cooled to 0 °C (ice water), and a needle was used to supply the gas mixture at a flow of 10–13 mL per min (monitored by a Porter B-125-6 flow-meter, Porter Instrument Company, Hatfield, PA, USA) for at least 30 min. Each solution was then allowed to equilibrate at the desired reaction temperature for an appropriate time period and the spectra were recorded at preselected time intervals while a gentle flow of the gas mixture was kept in the headspace of the cuvette.

The effect that $MbFe^{II}O_2$ has on $MbFe^{II}NO$ autoxidation was studied by using equimolar air-saturated solutions of $MbFe^{II}NO$ and $MbFe^{II}O_2$. Chilled solutions of each of the two purified species were adjusted to 1.00×10^{-5} M heme protein concentration using the extinction coefficients $\varepsilon_{MbNO,548}=12\,800$ and $\varepsilon_{MbO_2,544}=14\,400\,M^{-1}cm^{-1}$. Equal volumes of each were then mixed in a cuvette, which was equilibrated to a temperature of 30 °C, and the reaction was monitored spectrophotometrically as described above.

Determination of nitrite ions: To further elucidate the mechanism of $MbFe^{II}NO$ autoxidation at low and high pO_2, experiments were conducted to measure the amount of nitrite ions produced, if any, in solutions either saturated with 1% or 100% oxygen at 30 °C in air-tight test tubes. Each test tube was purged with the respective gas mixture during sampling, which was performed with a Hamilton syringe through a rubber septum. The method applied to quantify the nitrite ions was based on a standard colorimetric reaction of nitrite (Griess reagent) in acidified medium with detection at 543 nm.

Data handling: Recorded spectral data for $MbFe^{II}NO$ autoxidation at various temperatures and oxygen pressures were considered as a data matrix ($A_{m,n}$) that consisted of absorbance changes at m wavelengths and at n different time intervals. SVD was used as a standard mathematical method for reducing the dimensionality of the larger data sets because it has previously been successfully applied as a powerful tool for the evaluation of complex data sets obtained spectrophotometrically.[42,43] According to SVD theorem, a data matrix $A_{m,n}$ consists of the elements shown in Equation (9).

$$A_{m,n} = U_{m,n} \cdot S_{n,n} \cdot V^{T}_{n,n} \quad (9)$$

In Equation (9), U is an $m \times n$ orthogonal matrix that consists of n time-independent basic spectra, and S is an $n \times n$ diagonal matrix that contains the positive square roots of the eigenvalues (singular values) of A, ordered such that the significance of each component is represented (i.e. $S_{1,1} \geq S_{1,2} \cdots \geq 0$). Finally, V^T is an $n \times n$ orthogonal matrix, in which the rows contain time courses for each SVD component. The SVD data analysis for each data set was performed with the SPECFIT Global Analysis System Version 3.0.30 program (Spectrum Software Associates, Marlborough, MA, USA). The SVD results obtained from the spectral data were applied to global fitting with predefined kinetic models. The relevant concentration profiles and parameter estimates were obtained by the non-linear regression application of the Levenberg–Marquardt algorithm; this minimised the least-squares residuals and lead to refinement of the initial parameter estimates. Spectral data were analysed for two consecutive reactions using a kinetic model similar to the model applied by Arnold and Bohle.[17] The numerical values for the two rate constants obtained by regression analysis over the two consecutive reactions was based on calculations of the absorption spectrum for the corresponding intermediates. For each temperature and oxygen pressure, this analysis revealed a clear assignment based on "reasonable" absorption spectra without negative absorption regions. In experiments that investigated the effect of $MbFe^{II}O_2$ on the autoxidation rate of $MbFe^{II}NO$, inclusion of the pure prerecorded spectra for the two initial species was used in order to avoid rank deficiency (as a result of the presence of fewer "colours" than coloured species) in the SVD analysis, therby allowing parameter and concentration profiles to be estimated.

The observed rate constants determined at comparable experimental conditions were analysed by one-way ANOVA using the application Analyst within SAS systems statistical software release 8.02 (SAS Institute Inc., Cary, NC, USA).

Acknowledgements

This research was supported by the FøTEK program through LMC—Center for Advanced Food Studies. The authors would like to thank Dr. R. Bro, Royal Veterinary and Agricultural University, Department of Dairy and Food Science (Food Technology), and Dr. J.-P. Zhang, Institute of Chemistry, The Chinese Academy of Science, for their helpful discussions and advice in analysing the kinetic data. Furthermore, laboratory technician Lars Månsson is thanked for his skilful assistance during the experimental work in this study.

[1] D. J. Garry, G. A. Ordway, L. N. Lorenz, N. B. Radford, E. R. Chin, R. W. Grange, R. Bassel-Duby, R. S. Williams, *Nature* **1998**, *395*, 905–908.
[2] D. J. Garry, A. Meeson, Z. Yan, R. S. Williams, *Cell. Mol. Life Sci.* **2000**, *57*, 896–898.
[3] A. Godecke, U. Flogel, K. Zanger, Z. P. Ding, J. Hirchenhain, U. K. M. Decking, J. Schrader, *Proc. Natl. Acad. Sci. USA* **1999**, *96*, 10495–10500.
[4] U. Flogel, M. W. Merx, A. Godecke, U. K. M. Decking, J. Schrader, *Proc. Natl. Acad. Sci. USA* **2001**, *98*, 735–740.
[5] M. Brunori, *Trends Biochem. Sci.* **2001**, *26*, 209–210.
[6] M. Brunori, *Trends Biochem. Sci.* **2001**, *26*, 21–23.
[7] H. Frauenfelder, B. H. McMahon, R. H. Austin, K. Chu, J. T. Groves, *Proc. Natl. Acad. Sci. USA* **2001**, *98*, 2370–2374.
[8] G. C. Brown, *Biochim. Biophys. Acta* **1999**, *1411*, 351–369.
[9] G. C. Brown, *Acta Physiol. Scand.* **2000**, *168*, 667–674.
[10] C. E. Cooper, *Biochim. Biophys. Acta* **1999**, *1411*, 290–309.
[11] P. Ascenzi, M. Brunori, *Biochem. Mol. Biol. Educ.* **2001**, *29*, 183–185.
[12] P. K. Witting, D. J. Douglas, A. G. Mauk, *J. Biol. Chem.* **2001**, *276*, 3991–3998.
[13] G. G. Griddings, *Crit. Rev. Food Sci. Nutr.* **1977**, *9*, 81–111.
[14] L. H. Skibsted, A. Mikkelsen, G. Bertelsen, *Flavors of Meat, Meat Products and Seafoods*, (Eds.: F. Shahidi], Blackie Academic & Professional, London, UK, **1994**, pp. 217–256.
[15] L. H. Skibsted, *The Chemistry of Muscle-based Foods*, (Eds.: D. E. Johnston, M. K. Knight, D. A. Ledward], The Royal Society of Chemistry, Cambridge, UK, **1992**, pp. 266–286.
[16] J. K. S. Møller, L. Sosniecki, L. H. Skibsted, *Biochim. Biophys. Acta* **2002**, *1570*, 129–134.
[17] E. V. Arnold, D. S. Bohle, *Methods Enzymol.* **1996**, *269*, 41–55.
[18] R. F. Eich, T. S. Li, D. D. Lemon, D. H. Doherty, S. R. Curry, J. F. Aitken, A. J. Mathews, K. A. Johnson, R. D. Smith, G. N. Phillips, J. S. Olson, *Biochemistry* **1996**, *35*, 6976–6983.
[19] H. J. Andersen, L. H. Skibsted, *J. Agric. Food Chem.* **1992**, *40*, 1741–1750.
[20] J. K. S. Møller, L. H. Skibsted, *Chem. Rev.* **2002**, *102*, 1167–1178.
[21] J. H. Espenson, *Chemical Kinetics and Reaction Mechanisms*, McGraw-Hill, New York, USA, **1995**.
[22] S. Herold, *FEBS Lett.* **1998**, *439*, 85–88.
[23] S. Herold, M. Exner, T. Nauser, *Biochemistry* **2001**, *40*, 3385–3395.
[24] H. J. Andersen, G. Bertelsen, L. H. Skibsted, *Acta Chem. Scand.Acta Chem. Scand.!* **1988**, *42*, 226–236.
[25] D. A. Wink, J. Beckman, P. C. Ford, *Methods in Nitric Oxide Research* (Eds.: M. Feelisch, J. S. Stamler), Wiley, Chichester, UK, **1996**, pp. 29–37.
[26] R. F. Eich, *Reactions of nitric oxide with myoglobin*, Ph. D. dissertation, Rice University, Houston, TX, **1997**, pp. 100–111.
[27] E. G. Moore, Q. H. Gibson, *J. Biol. Chem.* **1976**, *251*, 2788–2794.
[28] V. G. Kharitonov, V. S. Sharma, D. Magde, D. Koesling, *Biochemistry* **1997**, *36*, 6814–6818.
[29] M. P. Doyle, J. W. Hoekstra, *J. Inorg. Biochem.* **1981**, *14*, 351–358.
[30] L. Bruun-Jensen, L. H. Skibsted, *Meat Sci.* **1996**, *44*, 145–149.
[31] S. Herold, *Arch. Biochem. Biophys.* **1999**, *372*, 393–398.
[32] H. J. Andersen, H. S. Johansen, C. K. Shek, L. H. Skibsted, *Z. Lebensm.-Unters. Forsch.* **1990**, *191*, 293–298.
[33] J. S. Olson, G. N. Phillips, *J. Biol. Chem.* **1996**, *271*, 17593–17596.
[34] K. Nakamura, K. Yokoyama, K. Nakamura, M. Itoman, *Scand. J. Plast. Reconstr. Surg. Hand Surg.* **2001**, *35*, 13–18.
[35] E. A. Konorev, J. Joseph, B. Kalyanaraman, *FEBS Lett.* **1996**, *378*, 111–114.
[36] A. L. Nakanishi, A. M. Roza, M. B. Adams, R. Seibel, G. Moore-Hilton, B. Kalyanaraman, G. M. Pieper, *Free Radical Biol. Med.* **1998**, *25*, 201–207.
[37] A. V. Gourine, A. A. Bulhak, A. T. Gonon, J. Pernow, P. O. Sjoquist, *Nitric Oxide* **2002**, *6*, 210–216.
[38] D. J. Garry, S. B. Kanatous, P. P. A. Mammen, *Trends Cardiovasc. Med.* **2003**, *13*, 111–116.
[39] M. Brunori, B. Vallone, F. Cutruzzola, C. Travaglini-Allocatelli, J. Berendzen, K. Chu, R. M. Sweet, I. Schlichting, *Proc. Natl. Acad. Sci. USA* **2000**, *97*, 2058–2063.
[40] M. Brunori, *Biophys. Chem.* **2000**, *86*, 221–230.
[41] M. Brunori, Q. H. Gibson, *EMBO Rep.* **2001**, *2*, 674–679.
[42] K. N. Walda, X. Y. Liu, V. S. Sharma, D. Magde, *Biochemistry* **1994**, *33*, 2198–2209.
[43] A. K. Dioumaev, *Biophys. Chem.* **1997**, *67*, 1–25.

Received: July 23, 2003
Revised: December 23, 2003 [F5368]